JOURNAL OF BACTERIOLOGY, Sept. 1996, p. 5417–5421 Vol. 178, No. 18
0021-9193/96/$04.00+0

Purification and Activation Properties of UreD-UreF-Urease Apoprotein Complexes

MARY BETH C. MONCRIEF AND ROBERT P. HAUSINGER*

Departments of Biochemistry and Microbiology, Michigan State University, East Lansing, Michigan 48824-1101

Received 10 April 1996/Accepted 9 July 1996

In vivo assembly of the *Klebsiella aerogenes* urease nickel metallocenter requires the presence of UreD, UreF, and UreG accessory proteins and is further facilitated by UreE. Prior studies had shown that urease apoprotein exists in an uncomplexed form as well as in a series of UreD-urease (I.-S. Park, M. B. Carr, and R. P. Hausinger, Proc. Natl. Acad. Sci. USA 91:3233–3237, 1994) and UreD-UreF-UreG-urease (I.-S. Park and R. P. Hausinger, J. Bacteriol. 177:1947–1951, 1995) apoprotein complexes. This study demonstrates the existence of a distinct series of complexes consisting of UreD, UreF, and urease apoprotein. These novel complexes exhibited activation properties that were distinct from urease and UreD-urease apoprotein complexes. Unlike the previously described species, the UreD-UreF-urease apoprotein complexes were resistant to inactivation by $NiCl_2$. The bicarbonate concentration dependence for UreD-UreF-urease apoenzyme activation was significantly decreased compared with that of the urease and UreD-urease apoproteins. Western blot (immunoblot) analyses with polyclonal anti-urease and anti-UreD antibodies indicated that UreD is masked in the UreD-UreF-urease complexes, presumably by UreF. We propose that the binding of UreF modulates the UreD-urease apoprotein activation properties by excluding nickel ions from binding to the active site until after formation of the carbamylated lysine metallocenter ligand.

Urease is a nickel-containing enzyme that catalyzes the hydrolysis of urea and serves as a virulence factor in microorganisms that are associated with urinary stone formation, gastric ulceration, and other human health concerns (2, 7). Crystallographic analysis of *Klebsiella aerogenes* urease revealed that the three structural subunits (encoded by *ureA*, *ureB*, and *ureC*) associate into a trimer of trimers [$(UreA\text{-}UreB\text{-}UreC)_3$] with each UreC subunit containing a novel bi-nickel metallocenter (3). The two nickel ions, separated by 0.35 nm, are bridged by a carbamylated lysine residue. Ni-1 is tricoordinate, bound by the carbamate and two histidine ligands, whereas Ni-2 is pentacoordinate, including the carbamate, two histidines, an aspartate, and a solvent molecule as ligands. The apoprotein, formed in cells grown in the absence of nickel ion or generated in accessory gene deletion mutants (5), is nearly identical to holoprotein in structure but lacks the metal ions and the bound carbon dioxide.

K. aerogenes urease apoprotein, here termed Apo, can be partially activated in vitro by incubation with nickel ions in bicarbonate-containing buffers (14). Carbon dioxide, in equilibrium with bicarbonate, reversibly reacts with the active-site lysine residue to form the requisite carbamate ligand. The concentration of carbon dioxide required for half-maximal activation is 0.2% or approximately sevenfold the atmospheric concentration of this gas. Under optimal conditions, only 10 to 15% of the Apo is activated. The activation reaction competes with nickel binding to noncarbamylated protein and with nonproductive nickel binding to carbamylated protein (15). An additional complication is that several other metal ions compete with nickel to form inactive metal-substituted species. Direct activation of Apo likely does not occur to any significant extent in the cell (reviewed in reference 8).

* Corresponding author. Mailing address: 160 Giltner Hall, Department of Microbiology, Michigan State University, East Lansing, MI 48824. Phone: (517) 353-9675. Fax: (517) 353-8957. Electronic mail address: RHausing@msu.edu.

Cellular activation of *K. aerogenes* urease requires the participation of three accessory proteins (UreD, UreF, and UreG) and is aided by a fourth (UreE) (5). These peptides are encoded by genes located in the same cluster (*ureDABCEFG*) as those encoding the enzyme subunits (5, 9). On the basis of its ability to bind nickel ions (6), UreE is suggested to play a role involving nickel donation or storage. In contrast, the other accessory proteins are thought to function as complexes with the urease subunits. Both *ureD* and *ureF* possess nonconsensus ribosome binding sites and are expressed at very low levels in the cell. Changing the ribosome binding site and initiation codon for *ureD* to yield a more-consensus-like sequence resulted in the synthesis of high levels of UreD, shown to be present in a series of complexes containing the trimeric Apo [$(UreA\text{-}UreB\text{-}UreC)_3$] binding one, two, or three UreD peptides (12). For convenience, these UreD-urease apoprotein complexes will be called D-Apo. Incubation of D-Apo with bicarbonate and nickel ions leads to UreD dissociation and partial activation, accounting for ~30% of the available apoprotein (14). As found for Apo, nonproductive reactions compete with the activation process. These reactions include nickel binding to noncarbamylated D-Apo, nickel binding improperly to the carbamylated species, and binding of other metal ions to form inactive metal-substituted proteins (15). The formation of D-Apo is not sufficient to account for activation of urease in the cell. Another series of Apo complexes containing UreD, UreF, and UreG has been detected and is able to be activated (13). Since all of these components are required for generating active urease in vivo, the UreD-UreF-UreG-Apo complexes (DFG-Apo) were suggested to serve as the key cellular urease activation machinery. These complexes are present at minute levels in the cell, and their properties have not been well characterized (11). The specific roles for UreD, UreF, and UreG in these complexes are unknown.

To better define the functions of the individual accessory proteins, we have identified, purified, and characterized the properties of a new series of complexes consisting of UreD,

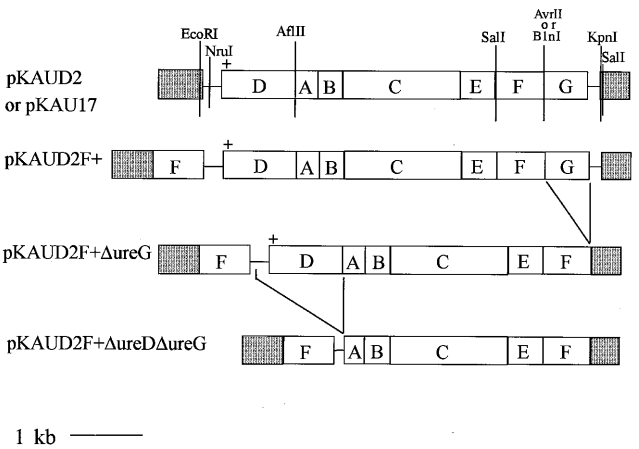

FIG. 1. Schematic representations of several plasmids utilized in these studies. The pKAUD2 or pKAU17 map shows several restriction sites used for plasmid constructions as well as the gene arrangements in the plasmids. Transcription proceeds from left to right. Note that pKAUD2 (12) is identical to pKAU17 (10), except that it is modified in the *ureD* ribosome binding site region and initiation codon to overexpress *ureD* (indicated by a +). The pUC8 vector is indicated (▤).

UreF, and the urease subunits. The UreD-UreF-Apo complexes (DF-Apo) have activation properties that are distinct from those of Apo or D-Apo species and provide insight into the role of UreF.

MATERIALS AND METHODS

Bacterial strains and plasmid construction. All molecular biology methods followed the general protocols outlined in Sambrook et al. (16).

Three constructs were generated in which *ureF* was overexpressed in a background containing all or most of the other urease genes, with *ureD* also expressed at high levels in two cases (Fig. 1). First, the 1.68-kbp *Sal*I fragment of pKAU17 (10) was blunt ended with Klenow fragment and ligated to phosphorylated *Nde*I linker (5′-ACCATATG-3′). The resulting product was digested with *Nde*I and *Avr*II, and the 670-bp fragment was ligated to the 5.7-kbp *Nde*I-*Nhe*I fragment of pET-11a (Novagen, Inc., Madison, Wis.), thus placing *ureF* under the control of the T7 promoter. This construct, pETF, was transformed into *Escherichia coli* BL21 (DE3) (Novagen). The 740-bp *Xba*I-*Bam*HI fragment of pETF was inserted into the blunt-ended *Eco*RI site of pKAUD2 (12) to form pKAUD2F+. A *ureG* deletion derivative of this plasmid, pKAUD2F+Δ*ureG*, was obtained by religation of the blunt-ended 8-kbp *Avr*II-*Kpn*I fragment. The double deletion mutant, pKAUD2F+Δ*ureD*Δ*ureG*, was constructed by digesting plasmid pKAUD2F+Δ*ureG* with *Nru*I and *Afl*II, filling in the *Afl*II 5′ overhang, and ligating the 7.1-kbp fragment ends. These plasmids were transformed into *E. coli* DH5α.

Culture conditions and cell disruption. *E. coli* DH5α(pKAUD2F+) or its derivatives were grown at 30 or 37°C to the late stationary phase in Luria-Bertani (LB) broth supplemented with 100 μg of ampicillin per ml, harvested by centrifugation, and suspended in PEDG (18 mM potassium phosphate [pH 7.4], 0.09 mM EDTA, 0.09 mM dithiothreitol, 10% glycerol) buffer. Resuspended cells were disrupted by two to three passages through a French pressure cell at 18,000 lb/in^2 (1 lb/in^2 = 6.89 kPa), supplemented with 1 mM phenylmethylsulfonyl fluoride, and separated into extracts and pellet fractions by centrifugation at 100,000 × *g* for 45 min at 4°C.

Purification of DF-Apo. Starting with *E. coli* DH5α(pKAUD2F+Δ*ureG*) cell extracts, DF-Apo was purified by successive chromatography on DEAE-Sepharose, Mono Q, and Superose 6 resins. The sample was applied to a DEAE-Sepharose column (2.5 by 19 cm; Pharmacia Biotech) equilibrated in PEDG buffer, and proteins were eluted from the column with a 400-ml linear salt gradient to 0.5 M KCl in the same buffer. Fractions containing DF-Apo were pooled, dialyzed against PEDG buffer, and applied to a Mono Q HR 10/10 (Pharmacia Biotech) column equilibrated with the same buffer. The proteins were eluted with a linear salt gradient to 1 M KCl in PEDG buffer. DF-Apo eluted from the column at 0.4 to 0.6 M KCl. Fractions containing the desired proteins were pooled, dialyzed against 18 mM phosphate (pH 7.4) buffer containing 0.09 mM EDTA, 0.09 mM dithiothreitol, and 0.1 M KCl. The protein pool was concentrated in a Centriprep-10 or -30 (Amicon, Beverly, Mass.) to 4 ml and chromatographed, via two runs, on a Superose 6 column (1.6 by 49 cm; Pharmacia Biotech) equilibrated in the same buffer.

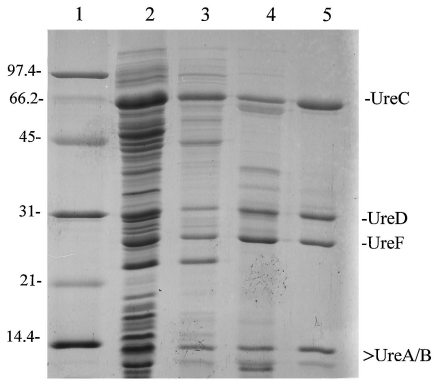

FIG. 2. Partial purification of the DF-Apo as analyzed by SDS-polyacrylamide gel electrophoresis. Lanes: 1, molecular weight markers (phosphorylase *b*, M_r 97,400; bovine serum albumin, M_r 66,200; ovalbumin, M_r 45,000; carbonic anhydrase, M_r 31,000; soybean trypsin inhibitor, M_r 21,000; lysozyme, M_r 14,400); 2, *E. coli* DH5α(pKAUD2F+Δ*ureG*) cell extracts; 3, DEAE-Sepharose pool; 4, Mono Q pool; 5, Superose 6 pool.

Polyacrylamide gel electrophoresis. Sodium dodecyl sulfate (SDS)-polyacrylamide gel electrophoresis was carried out with the buffers described by Laemmli (4) and included 4.5 and 13.5% polyacrylamide stacking and running gels. Nondenaturing gels used the same buffers without detergent and consisted of 3 and 6% polyacrylamide stacking and running gels. The gels were either stained with Coomassie brilliant blue or electroblotted onto nitrocellulose, probed with anti-*K. aerogenes* urease antibodies (10) or anti-*K. aerogenes* UreD antibodies (17), and visualized by use of anti-rabbit immunoglobulin G-alkaline phosphatase conjugates (1). The band intensities of Coomassie blue-stained gels were determined with an AMBIS (San Diego, Calif.) gel scanner. For calculation of the ratios of UreD, UreF, and UreC, M_r values of 29,300, 27,000, and 60,300 were used.

Urease activity assays. Urease activity was measured by quantitating the rate of ammonia release from urea by formation of indophenol, which was monitored at 625 nm (19). One unit of urease activity was defined as the amount of enzyme required to hydrolyze 1 μmol of urea per min at 37°C. The standard assay buffer consisted of 25 mM HEPES (*N*-2-hydroxyethylpiperazine-*N*′-2-ethanesulfonic acid; pH 7.75), 0.5 mM EDTA, and 50 mM urea. Protein concentrations were determined by a commercial assay (Bio-Rad, Hercules, Calif.) with a bovine serum albumin standard.

Activation of urease apoproteins. Routine Apo, D-Apo, and DF-Apo activation buffer consisted of 100 mM HEPES (pH 8.3), 150 mM NaCl, 100 mM $NaHCO_3$, and 100 μM $NiCl_2$ (15). For specific experiments, the conditions were modified by varying the bicarbonate or nickel ion concentrations, adding other metal ions to the activation buffer, or incubating samples in the presence of metal ions prior to addition of bicarbonate.

RESULTS AND DISCUSSION

Purification and characterization of UreD-UreF-urease apoprotein complexes. *E. coli* DH5α(pKAUD2F+Δ*ureG*) synthesized high levels of the urease subunits, UreD, and UreF. When peptides from cells that were grown in the absence of nickel ions were analyzed, they were found to copurify during DEAE-Sepharose, Mono Q, and Superose 6 chromatographies as illustrated by denaturing polyacrylamide gel electrophoretic analysis of the resulting protein pools (Fig. 2, lanes 2 to 5). On the basis of the staining intensities, the composition of the last pool was calculated to be 0.86 to 0.89 UreD and 0.78 to 0.81 UreF per UreC. The broad elution profile from the gel permeation column suggested that multiple DF-Apo species were present. Results from nondenaturing polyacrylamide gel electrophoretic analyses were consistent with the presence of three DF-Apo complexes when proteins were visualized by probing with anti-urease immunoglobulin G (Fig. 3A, lane 3). The electrophoretic migration positions of these complexes corresponded to those described previously for the D-Apo complexes (12), as shown in Fig. 3A, lane 2. Surprisingly,

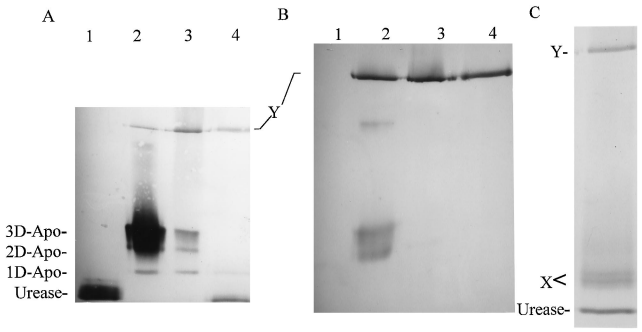

FIG. 3. Native polyacrylamide gel electrophoretic comparison of the D-Apo and DF-Apo samples. (A) Western blot analysis of a nondenaturing polyacrylamide gel visualized with anti-*K. aerogenes* urease antibodies. Lanes: 1, 10 μg of Apo; 2, 10 μg of D-Apo complexes; 3, 20 μg of DF-Apo; 4, 10 μg of DF-Apo complexes incubated in activation buffer at 37°C for 90 min. (B) Western blot comparison with anti-UreD antibodies for samples as described for lanes of panel A. (C) Coomassie blue-stained native gel with the same protein sample as that described for panel A, lane 4. The migration positions for Apo (Urease) and D-Apo containing 1, 2, and 3 UreD (1D-Apo, 2D-Apo, and 3D-Apo) per trimeric urease [(UreA-UreB-UreC)$_3$] (12) are indicated. The bands labelled X are from unidentified peptides that do not cross-react with anti-urease or anti-UreD antibodies. The band labelled Y contains GroEL that cross-reacts with anti-urease and anti-UreD antibodies.

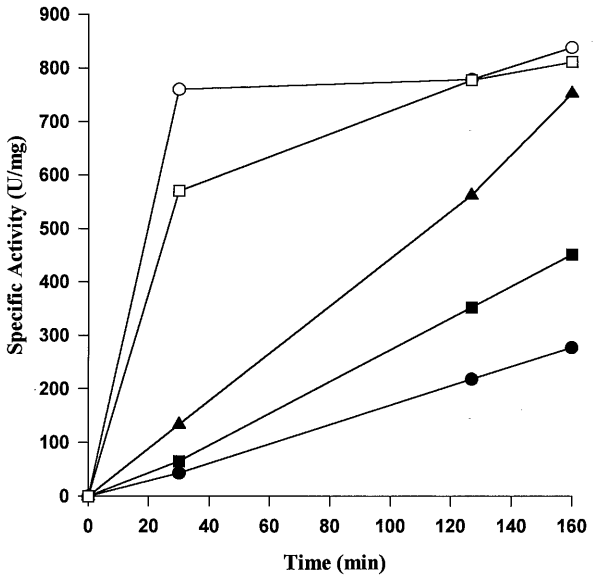

FIG. 4. Nickel ion concentration dependence of activation for DF-Apo. The purified sample (0.1 mg/ml) was incubated at 37°C in 100 mM HEPES (pH 8.3) buffer containing 150 mM NaCl, 100 mM $NaHCO_3$, and 25 (●), 50 (■), 100 (▲), 500 (○), or 1,000 (□) μM $NiCl_2$. Aliquots were removed at the indicated times, and the samples were assayed for urease activity.

however, anti-UreD antibodies failed to detect cross-reactive material associated with the DF-Apo bands (Fig. 3B, lane 3), whereas the D-Apo species were detected (Fig. 3B, lane 2). (When the same fractions were analyzed by Western blot [immunoblot] analysis of a denaturing gel, UreD was clearly detected by these antibodies [data not shown].) After incubation with nickel ions in activation buffer, the three DF-Apo species collapsed to form a band that migrated at the position of urease and Apo (Fig. 3A, lane 4, and Fig. 3C), similar to the results reported for D-Apo (12). Addition of bicarbonate alone had no effect on the band migration. Two bands (labelled X in Fig. 3) that migrated more slowly than urease but slightly faster than the one D-Apo species were detected by Coomassie blue staining of the activated DF-Apo species. These bands did not cross-react with anti-urease or anti-UreD antibodies. As observed previously for cell extracts from *E. coli* DH5(pKAU17) (13), a slowly migrating band (labelled Y in Fig. 3) cross-reacted with anti-urease and anti-UreD antibodies. Two-dimensional gels (data not shown) indicated that the predominant protein in this band is that visible just below UreC in Fig. 2. N-terminal sequence analysis of this peptide revealed a sequence consistent with that of GroEL (XXKDVKF). Purified *E. coli* GroEL was found to electrophorese at positions corresponding to these bands on native and denaturing gels, and both antibodies were observed to cross-react with authentic GroEL. We conclude that GroEL is present at substoichiometric levels in our preparations of D-Apo and DF-Apo.

From the results described above, we conclude that the DF-Apo species represent the trimeric urease apoprotein [(UreA-UreB-UreC)$_3$] with one, two, or three each of UreD and UreF peptides bound. On the basis of Western blot analyses, we suggest that the UreF peptides mask the UreD peptides, i.e., anti-UreD antibodies fail to detect the UreD that is present in DF-Apo, although the peptide is recognized in D-Apo. Although DF-Apo and D-Apo complexes appear to migrate identically when examined by native gel electrophoresis, slight changes in size are detected when these samples are examined by gel permeation chromatography. It is likely that the DF-Apo complexes were unknowingly observed before. In prior studies that sought to examine the requirements for D-Apo formation, deletion mutants in *ureE*, *ureF*, or *ureG* were studied by immunological methods with *E. coli* cells containing the *K. aerogenes* urease gene cluster (13). Although the D-Apo complexes in Δ*ureF* mutant cells comigrated with complexes from control and Δ*ureE* or Δ*ureG* mutant cells during electrophoresis, the absence of UreF led to an apparent diminishment in gel chromatography size that was attributed to a conformational change induced by UreF. The present findings allow us to reinterpret the prior results: the control and Δ*ureE* or Δ*ureG* mutants actually formed DF-Apo, and only the Δ*ureF* mutant cells formed D-Apo.

To examine whether UreD was needed for UreF to form a complex with the urease subunits, pKAUD2F + Δ*ureD*Δ*ureG* was constructed. Cells containing this plasmid were disrupted, and extracts were chromatographed on DEAE-Sepharose and Mono Q columns. The urease subunits eluted from these resins as noncomplexed species, and UreF appeared to be almost entirely insoluble. Furthermore, when *ureF* was expressed separately from the genes encoding the urease subunits, the gene product was located exclusively in the insoluble fraction (data not shown).

Activation properties of DF-Apo. When standard Apo activation conditions were used, the DF-Apo pool was activated to a specific activity value of 800 ± 100 U/mg of total protein (e.g., see closed triangles in Fig. 4 and Fig. 5A). This level of activation was very similar to that observed for D-Apo and about twice that obtained for Apo (14, 15). For comparison, native urease isolated from *K. aerogenes* possesses a specific activity of ~2,500 U/mg of protein (18). The rate of DF-Apo activation, however, was significantly lower than that observed with either of the other apoproteins when assessed under similar conditions. For example, 60 to 90 min was required for half-maximal activation of DF-Apo, compared with 15 to 20 min for the Apo and D-Apo species (14).

The nickel and bicarbonate concentration dependencies were significantly altered for the new species compared with the corresponding properties for Apo and D-Apo. As shown in

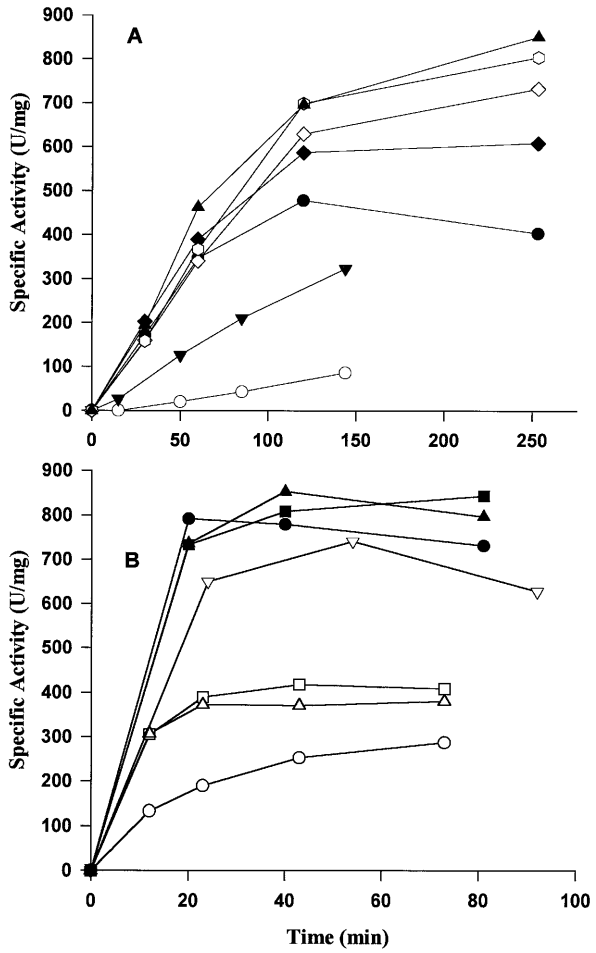

FIG. 5. Bicarbonate ion concentration dependence of activation for DF-Apo. The sample (0.1 mg/ml) was incubated at 37°C in 100 mM HEPES (pH 8.3) buffer containing 150 mM NaCl, 100 (A) or 500 (B) μM $NiCl_2$, and the following concentrations of added $NaHCO_3$: 0 (○), 0.1 (△), 0.25 (□), 1 (▽), 2 (▼), 5 (●), 10 (◆), 25 (◇), 50 (■), 75 (○), or 100 (▲) mM.

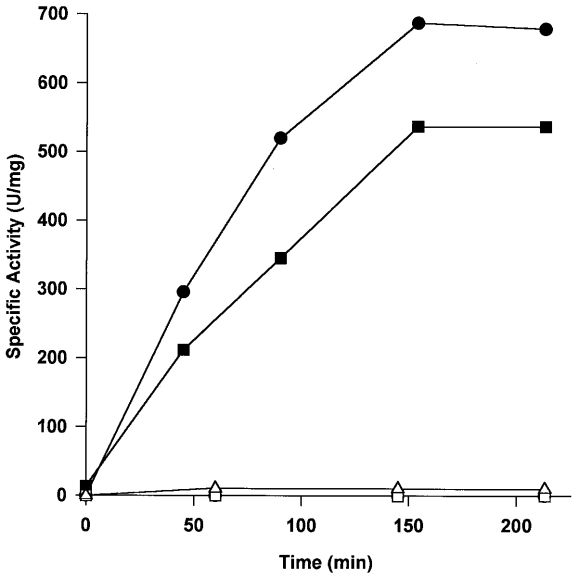

FIG. 6. Effect of incubation of DF-Apo with metal ions prior to activation by $NiCl_2$ and bicarbonate. The sample (0.5 mg/ml) was incubated at 37°C in buffer containing 100 mM HEPES (pH 8.3) and 150 mM NaCl with no metal (●) or with 100 μM $NiCl_2$ (■), $ZnCl_2$ (○), $CoCl_2$ (△), or $CuCl_2$ (□). After 80 min, an aliquot of each mixture was activated in 100 mM HEPES (pH 8.3) buffer containing 150 mM NaCl, 100 μM $NiCl_2$, and 100 mM $NaHCO_3$, and samples were assayed for urease at the indicated time points.

Fig. 4, the nickel ion concentration exhibited a marked effect on the DF-Apo activation rate, with increasing rates observed to 500 μM $NiCl_2$ and slight inhibition observed at 1 mM $NiCl_2$. In contrast, the Apo and D-Apo species exhibit maximal activation rates at ~60 μM $NiCl_2$ and are inhibited by nickel ion concentrations above 300 μM (14). For DF-Apo, half-maximal levels of activity were achieved at ~5 mM added bicarbonate when 100 μM $NiCl_2$ (Fig. 5A) was used or at ~250 μM sodium bicarbonate when 500 μM $NiCl_2$ (Fig. 5B) was used. These results contrast those obtained with Apo and D-Apo species, which exhibit half-maximal activation in the presence of approximately 10 mM bicarbonate.

As another measure to compare activation properties of DF-Apo versus Apo and D-Apo species, the ability for various metal ions to inhibit the activation process was studied. Prior incubation of DF-Apo with nickel ions in the absence of added bicarbonate led to only a slight reduction in its ability to be activated (Fig. 6). Prior work demonstrated that these same conditions greatly reduced the activation competence of Apo and D-Apo (15). On the other hand, DF-Apo was almost completely inhibited by prior incubation with 100 μM zinc, cobalt, or copper ions (Fig. 6), similar to the behavior of Apo and D-Apo samples (15). As observed with the previously characterized species, inhibition of DF-Apo resulted when activation was carried out with buffers containing 100 or 500 μM $NiCl_2$ and varied concentrations of zinc ions (Fig. 7). For example, only about 50% of the urease in the pool was activated with 100 μM $NiCl_2$ in the presence of ~3.3 μM zinc ions. In the presence of 500 μM $NiCl_2$, a slightly higher concentration of zinc ion (4.3 μM) was required to inhibit activation by 50%.

Function of UreF. The enhanced activation properties of DF-Apo over D-Apo and Apo (i.e., an increased resistance to nickel ion inhibition and a decreased bicarbonate concentration dependence) provide compelling evidence that this novel complex is biologically relevant. Although DF-Apo may not exist to any significant extent in the cell, it may occur as an intermediate to formation of the DFG-Apo species and it appears to provide insight into the role of UreF. We propose that UreF modulates the activation process primarily by eliminating the binding of nickel ions to noncarbamylated protein. This change greatly facilitates formation of the carbamylated protein, which in turn results in a lowered bicarbonate requirement. As in the Apo and D-Apo species (15), however, the carbamylated DF-Apo protein is likely to bind nickel ion to yield two states, only one of which is active. Thus, in vitro activation of DF-Apo yields a final specific activity that falls far short of that observed (~2,500 U/mg) in fully active enzyme (18). The ratio of active to inactive nickel-containing carbamylated protein arising from DF-Apo is likely to be similar to that generated from D-Apo, on the basis of their similar final specific activities of ~800 U/mg of total protein. In addition to eliminating the interaction of nickel ions with noncarbamylated urease apoprotein, an added consequence of forming the DF-Apo is to reduce the overall activation rate by approximately fivefold. Additional studies are needed to elucidate how UreF acts to preclude nickel ion from binding to the noncarbamylated apoenzyme complex and why zinc, cobalt, and copper ions do not appear to be similarly excluded. Furthermore,

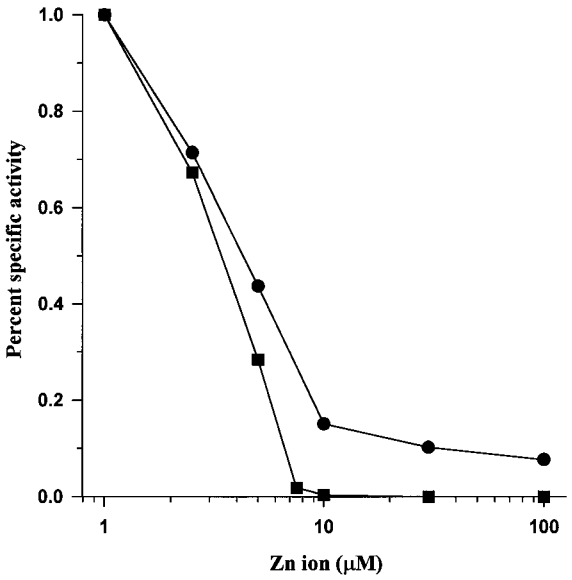

FIG. 7. Effect of zinc ion concentration on DF-Apo activation. The sample (0.1 mg/ml) was incubated in activation buffer containing 100 (■) or 500 (●) μM $NiCl_2$ and the indicated concentrations of $ZnCl_2$. The percent specific activity, based on a sample containing no zinc ions, was determined after 4 h of incubation.

it will be important to purify the DFG-Apo species and characterize how its activation properties compare with those of Apo, D-Apo, and now DF-Apo.

ACKNOWLEDGMENTS

We thank Matt Todd for providing a sample of GroEL and members of the laboratory for their comments and suggestions concerning the manuscript.

This work was supported by the National Institutes of Diabetes and Digestive and Kidney Diseases (DK45686) and by the Michigan State University Agricultural Experiment Station.

REFERENCES

1. **Blake, M. S., K. H. Johnston, G. L. Russel-Jones, and E. C. Gotschlich.** 1984. A rapid, sensitive method for detection of alkaline phosphatase-conjugated anti-antibody on Western blots. Anal. Biochem. **136:**175–179.
2. **Hausinger, R. P.** 1993. Urease, p. 23–57. *In* Biochemistry of nickel. Plenum Publishing Corp., New York.
3. **Jabri, E., M. B. Carr, R. P. Hausinger, and P. A. Karplus.** 1995. The crystal structure of urease from *Klebsiella aerogenes*. Science **268:**998–1004.
4. **Laemmli, U. K.** 1970. Cleavage of structural proteins during the assembly of the head of bacteriophage T4. Nature (London) **227:**680–685.
5. **Lee, M. H., S. B. Mulrooney, M. J. Renner, Y. Markowicz, and R. P. Hausinger.** 1992. Sequence of *ureD* and demonstration that four accessory genes (*ureD*, *ureE*, *ureF*, and *ureG*) are involved in nickel metallocenter biosynthesis. J. Bacteriol. **174:**4324–4330.
6. **Lee, M. H., H. S. Pankratz, S. Wang, R. A. Scott, M. G. Finnegan, M. K. Johnson, J. A. Ippolito, D. W. Christianson, and R. P. Hausinger.** 1993. Purification and characterization of *Klebsiella aerogenes* UreE protein: a nickel-binding protein that functions in urease metallocenter assembly. Protein Sci. **2:**1042–1052.
7. **Mobley, H. L. T., M. D. Island, and R. P. Hausinger.** 1995. Molecular biology of microbial ureases. Microbiol. Rev. **59:**451–480.
8. **Moncrief, M. B. C., and R. P. Hausinger.** 1996. Nickel incorporation into urease, p. 151–171. *In* R. P. Hausinger, G. L. Eichhorn, and L. G. Marzilli (ed.), Mechanisms of metallocenter assembly. VCH Publishers, New York.
9. **Mulrooney, S. B., and R. P. Hausinger.** 1990. Sequence of the *Klebsiella aerogenes* urease genes and evidence for accessory proteins facilitating nickel incorporation. J. Bacteriol. **172:**5837–5843.
10. **Mulrooney, S. B., H. S. Pankratz, and R. P. Hausinger.** 1989. Regulation of gene expression and cellular localization of cloned *Klebsiella aerogenes* (*K. pneumoniae*) urease. J. Gen. Microbiol. **135:**1769–1776.
11. **Park, I.-S.** 1994. Ph.D. thesis. Michigan State University, East Lansing.
12. **Park, I.-S., M. B. Carr, and R. P. Hausinger.** 1994. *In vitro* activation of urease apoprotein and role of UreD as a chaperone required for nickel metallocenter assembly. Proc. Natl. Acad. Sci. USA **91:**3233–3237.
13. **Park, I.-S., and R. P. Hausinger.** 1995. Evidence for the presence of urease apoprotein complexes containing UreD, UreF, and UreG in cells that are competent for in vivo enzyme activation. J. Bacteriol. **177:**1947–1951.
14. **Park, I.-S., and R. P. Hausinger.** 1995. Requirement of carbon dioxide for in vitro assembly of the urease nickel metallocenter. Science **267:**1156–1158.
15. **Park, I.-S., and R. P. Hausinger.** 1996. Metal ion interactions with urease and UreD-urease apoproteins. Biochemistry **35:**5345–5352.
16. **Sambrook, J., E. F. Fritsch, and T. Maniatis.** 1989. Molecular cloning: a laboratory manual, 2nd ed. Cold Spring Harbor Laboratory, Cold Spring Harbor, N.Y.
17. **Taha, T., and R. P. Hausinger.** 1996. Unpublished observations.
18. **Todd, M. J., and R. P. Hausinger.** 1987. Purification and characterization of the nickel-containing multicomponent urease from *Klebsiella aerogenes*. J. Biol. Chem. **262:**5963–5967.
19. **Weatherburn, M. W.** 1967. Phenol-hypochlorite reaction for determination of ammonia. Anal. Chem. **39:**971–974.